Effect of equal channel angular pressing process on drawability of DC04 steel sheets

M. Talantikite [a,*], A. Mebarek [a], M.Zaaf [a], S. Boukeffa [b]

[a] Laboratory of Metal Materials Forming (LMF2M), Faculty of Technology, Badji Mokhtar-Annaba University, Annaba, Algeria

[b] Materials Physico-Chemistry Laboratory (LPCM), Physics Department, Science and Technology Faculty, Eltarf University, Eltarf, Algeria

*Correspondence: talantikitemassil99@gmail.com

abmebarek@yahoo.fr, zaaf_mohamed@yahoo.fr, wassilmss@yahoo.fr

(Received 19 May 2024; Accepted 10 February 2025)

Abstract:

Equal channel angular pressing (ECAP) is a severe plastic deformation (SPD) technique that induces substantial changes in the crystalline structure of materials, leading to enhanced mechanical properties. This experimental work aims to study the influence of ECAP on the drawability of DC04 steel sheets. A multilayered sample of six sheets was deformed at room temperature with an internal channel angle of 120° for a single pass. Characterization was conducted by measuring hardness and performing tensile tests, along with optical microscopy and X-ray diffraction (XRD) analysis. Additionally, finite element simulation using Abaqus was implemented. The Erichsen test was employed to assess the drawability of the sheet exhibiting the best mechanical properties. The results indicated a significant increase in microhardness, with an improvement of 64% compared to the original microhardness. Microstructural analysis revealed a 70% reduction in grain size, with slight texture formation and no phase change. Tensile tests showed an increase in yield stress (Re) and ultimate tensile strength (Rm), accompanied by a decrease in elongation (A%) and strain hardening exponent (n). The Erichsen test demonstrated a slight 10% reduction in the Erichsen cupping index (IE). Overall, we successfully enhanced the mechanical properties of the DC04 steel plates while maintaining good drawability.

Keywords: ECAP, Drawability, Erichsen test, DC04 steel sheets, Simulation, Manufacturing technologies

1.Introduction:

In the field of metal forming, deep drawing is used in the manufacturing industry for the production of various components such as automobile bodies, aircraft panels, domestic appliance bodies, kitchen utensils, and beverage cans [1]. The ability of a material to undergo deep drawing is influenced by its inherent properties, determined by its chemical composition and structure [2]. Advanced processing techniques can achieve changes in these properties. ECAP is defined as a method of severe plastic deformation (SPD). This method is an innovative one invented and explained by Segal and developed by Valiev [3] and Langdon [4], which details the principle of ECAP and the influence of different parameters.

The DC04 is a deep-drawing steel suitable for the high requirements of forming. It mainly has potential for light structural applications in the automotive and aerospace industries. This is due to properties such as reasonable strength and ductility [5-6].

The scientific literature attests to a growing interest in the recent application of the ECAP

process to improve the mechanical properties of materials. This improvement is achieved through the significant refinement of grain sizes, leading to the formation of ultrafine grains. Fukuda et al. [7] conducted a study on the influence of ECAP on cylindrical low-carbon steel billets with a section of 10 mm in diameter and a length of 60 mm. This study was carried out using route Bc in a canal with an interior angle (Θ) of 90° and an exterior angle (Ψ) of 20°.The results demonstrated a reduction in grain size, leading to an increase in yield strength and ultimate tensile strength, accompanied by a decrease in elongation percentage. A. Chandra et al. [8] also worked with low carbon steel (0.2% by weight of C). The specimen used has a diameter of 12 mm and a length of 60 mm. ECAP process parameters were set at Θ=120° and Ψ=20°, with a temperature range varying from 200 to 350 °C. A significant increase in Vickers hardness from 133 to 269 HV was observed, accompanied by a notable increase in tensile strength of about 2.2 times. However, the elongation decreased from 51% to 13%. M. Eddahbi et al. [9] examined the influence of (ECAP) on EUROFER 97 steel billets; EUROFER97 is the European Reduced Activation Ferritic-Martensitic (RAFM) steel, having dimensions of 12 mm × 12 mm × 65 mm. The ECAP was carried out at a temperature of 550°C with an angle of 105° following route C. The conclusions of this study indicate an improvement in the mechanical behavior of this steel. This improvement is attributed to the grain refinement and texture evolution of the lamellar substructure induced by ECAP deformation, M. B. Jabłońska et al. [10] examined the effect of the Dual Roll Equal Channel Extrusion (DRECE) method on IF steel strips measuring 800 mm in length, 60 mm in width, and 2 mm in thickness. Their study demonstrated that after four DRECE passes, the fraction of low-angle grain boundaries (LAGBs) significantly increased from 7% in the initial sample to 54%. With an increase in the number of passes, the mechanical properties improved, with the yield strength reaching a maximum of 328 MPa after seven DRECE passes. However, the elongation to failure decreased significantly, from 46% in the as-received condition to 13% after seven DRECE passes, K. Kowalczyk et al. [11] focused on the effect of DRECE method on DC01 steel with dimension of 800 x 60 x 2 mm, after multiple DRECE passes, there is a marked increase in the formation of low-angle subgrain boundaries, reaching 51% after seven passes, indicating advanced microstructural transformation towards high-angle boundaries, Additionally, microhardness measurements reveal a significant increase in hardness with each pass, indicating material hardening and improved homogeneity.

On the other hand, the influence of ECAP on the drawability of low carbon steel DC04 has not yet been studied. Existing literature, such as the work of J. Suh et al. [12] on the impact of different ECAP routes (A, C, and D) on the texture and cold formability of AZ31 sheets, H.R. Rahimi et al. [13] on Al-Mg alloy plate (5083) using the ECAR process, and M. Ciemiorek et al. [14] on commercial alloy 3003 plates using Incremental ECAP, primarily focus on different materials and process modifications. These studies, while valuable, highlight the need for further research specific to low carbon steel DC04.

2. Material and methods:

In this study, experimental trials were undertaken using an ECAP die. This die was designed at the Metal Materials Forming Laboratory (LMF2M) at Badji Mokhtar Annaba University to assess the impact of this technique on the mechanical properties and drawability of DC04 steel sheets. This investigation took place in two distinct phases. Initially, attention was paid to the influence of ECAP on the microstructure and mechanical properties of DC04 steel sheets. Subsequently, a study of drawability was conducted specifically on the sheet with optimal properties using the Erichsen test. These results contribute to understanding the effect of ECAP on the mechanical performance and drawability of DC04 steel sheets, offering perspectives for its application in forming processes.

2.1 Material:

The material used in this study is low carbon steel DC04, developed at the SIDER El-Hadjar steel complex in Annaba. The latter is supplied in the form of cold rolled 1.5 mm thick sheets that are then annealed. Its chemical composition, obtained by spectroscopy, is recorded in Table 1.

Elements	C	Mn	Cu	Al	Ni	Cr
wt%	0,06	0,19	0,04	0,081	0,01	0,01

Table 1 chemical composition of DC04.

2.2 Methodology and experimentation:

Figure 1 shows the ECAP die used in our study. The die consists of a central part and an auxiliary part machined from 55NCDV7 steel, quenched in oil, followed by tempering. The assembly of these two parts forms two channels with the same cross section of 10x120 mm, namely the inlet channel and the other outlet. These two channels are connected by an elbow having an interior angle Θ of 120° and an exterior angle Ψ of 10°, For the selection of the interior and exterior angles, we based our choice on the literature, where several studies have used these angles (120° and 10°). However, we are willing to use other angles [8,14,15] . Figure 2 shows samples before and after ECAP.

Figure 3.a illustrates the principle of the ECAP technique used. Six sheets of dimension 119.9x100 mm were previously cut and then placed in multilayered sample in the die, as shown in Figure 1.c. A punch with a rectangular section of 9.8x119.8 mm and a height of 100mm is used to extrude the sheets in the input channel, thus passing them through the elbow connecting the two channels. Figure 3.b shows the orientation of rolling direction (RD) versus metal flow in ECAP.

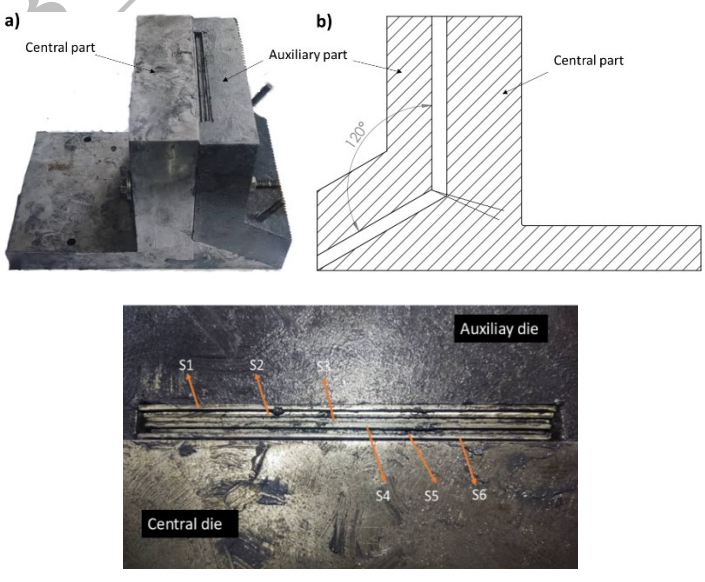

Fig. 1 a) ECAP die; b) ECAP die cross-section; c) Positioning of sheets inside channel.

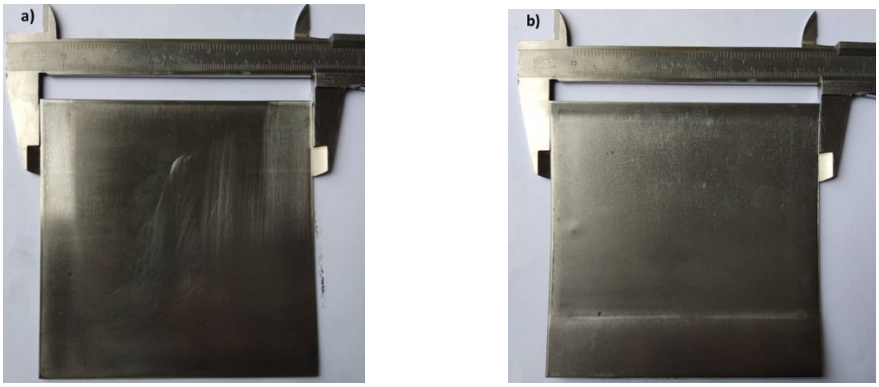

Fig 2 DC04 steel sheet a) before ECAP, b) S1 after ECAP

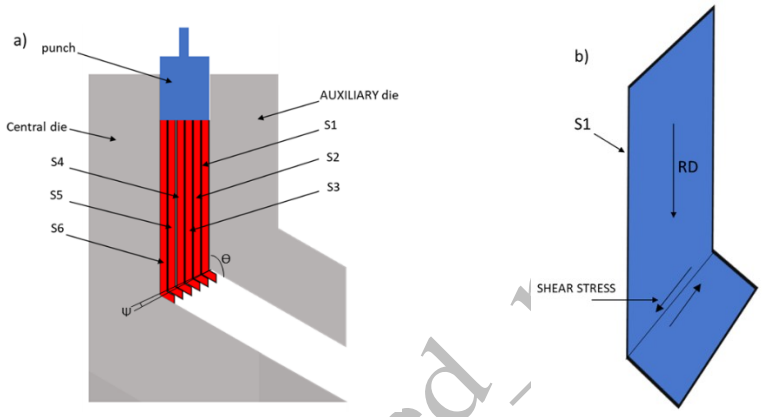

Fig. 3 a) schematic diagram of the ECAP process. b) rolling direction (RD) versus metal flow in ECAP

In order to reduce friction, a molybdenum disulfide-based lubricant (MoS_2) was applied to the entire channel and between the sheets. The (ECAP) process was performed for a single pass with an internal angle of 120° and a pressing speed maintained at 0.5 mm/s. Microhardness measurements were carried out using a ZWICK brand Vickers durometer, applying a load of 200 gf. A total of seventeen measurements were taken for each sheet, and their average was noted. The configuration of the measurement locations is shown in Figure 4.

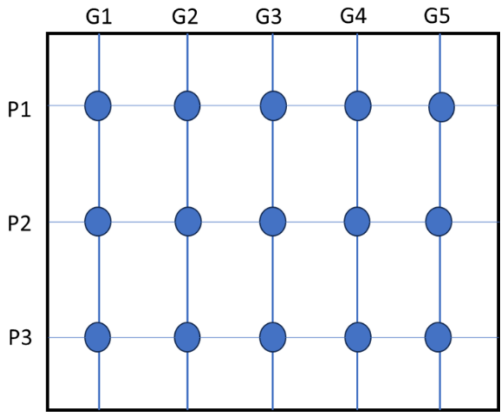

Fig. 4 Representation of the location of the 15 microhardness measurements.

2.3 Characterization of the microstructure:

After sequential mechanical polishing using SiC abrasive paper from 400 to 4000 grit, a 2% Nital solution was used as an etching agent to reveal the grain structure. Optical microscopy was used to observe the microstructure of the sheets before and after ECAP.

X-ray diffraction (XRD) measurements were carried out on the surface of the sheets before and after ECAP, with the aim of evaluating possible structural changes and analyzing any changes in the diffraction peaks. The D8 ADVANCE BRUKER diffractometer was used with Cu-Kα radiation (λ = 1.54 Å) and a pitch of 0.02°.

2.4 Tensile test:

To evaluate the mechanical properties of the sheets before and after the ECAP process, tensile tests were conducted using a ZWICK Z020 machine. The specimens were cut in the extrusion direction and dimensioned according to EN ISO 6892-1, as shown in Figure 5.

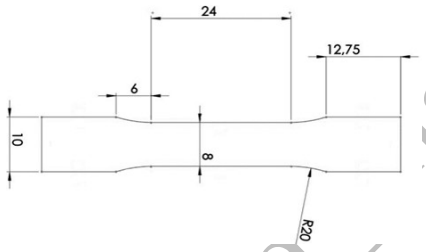

Fig. 5 Tensile test specimen according to EN ISO 6892-1.

2.5 Erichsen cup Test:

In order to assess the ductility and drawability of the sheets before and after ECAP, the Erichsen test was used in accordance with the standards DIN EN 10139 and DIN EN 10130.

The sheet to be stamped is fixed in a special hydraulic press, and a progressively increasing load is applied to the surface of the sheet by a hemispherical punch of 20mm diameter until a crack appears [17-18]. Figure 6 schematically illustrates the Erichsen test.

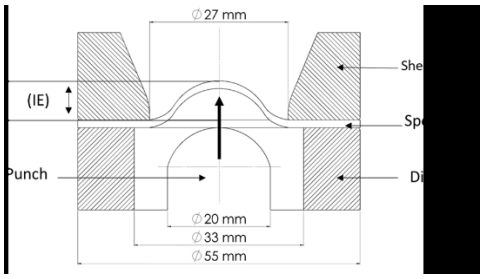

Fig. 6 schematic diagram of the Erichsen cup test**.**

The resulting deformation is measured in depth using a caliper and expressed in millimeters. The Erichsen index (IE) is calculated using the formula (Eq. (1)). A high Erichsen index (IE) indicates better ductility and drawability of the material.

$$\text{IE} = \text{depth of the cup} - \text{thickness of the sheet} \qquad (1)$$

The propagation and shape of the crack are also evaluated [19].

3 Results and discussions:

3.1 Effect of ECAP on microhardness:

The microhardness measurements, recorded in figure 7, show an increase in microhardness for all of the sheets after ECAP, thus highlighting the beneficial effect of ECAP. This increase can be attributed to grain refinement [10,19]. Position S1, which is in direct contact with the interior angle Θ of the die, exhibits the most significant increase, with a value of 64%. This result can be explained by the greater deformation of the sheet S1, which is in direct contact with the wall of the die. The other sheets show a moderate increase of around 13%. Also, all the sheets after ECAP show a reduction in the standard deviation, thus suggesting a homogenization of the microstructure [10,19].

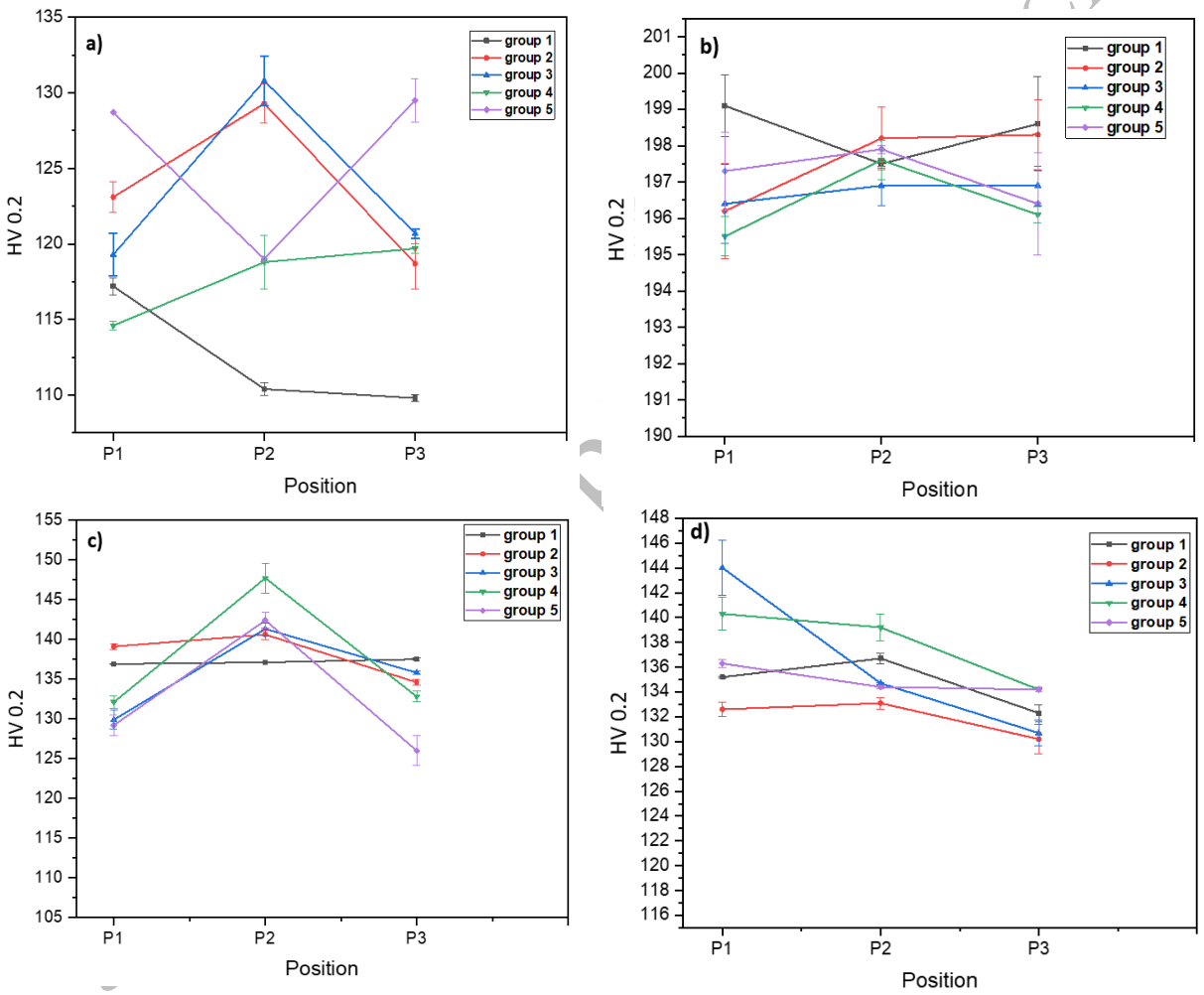

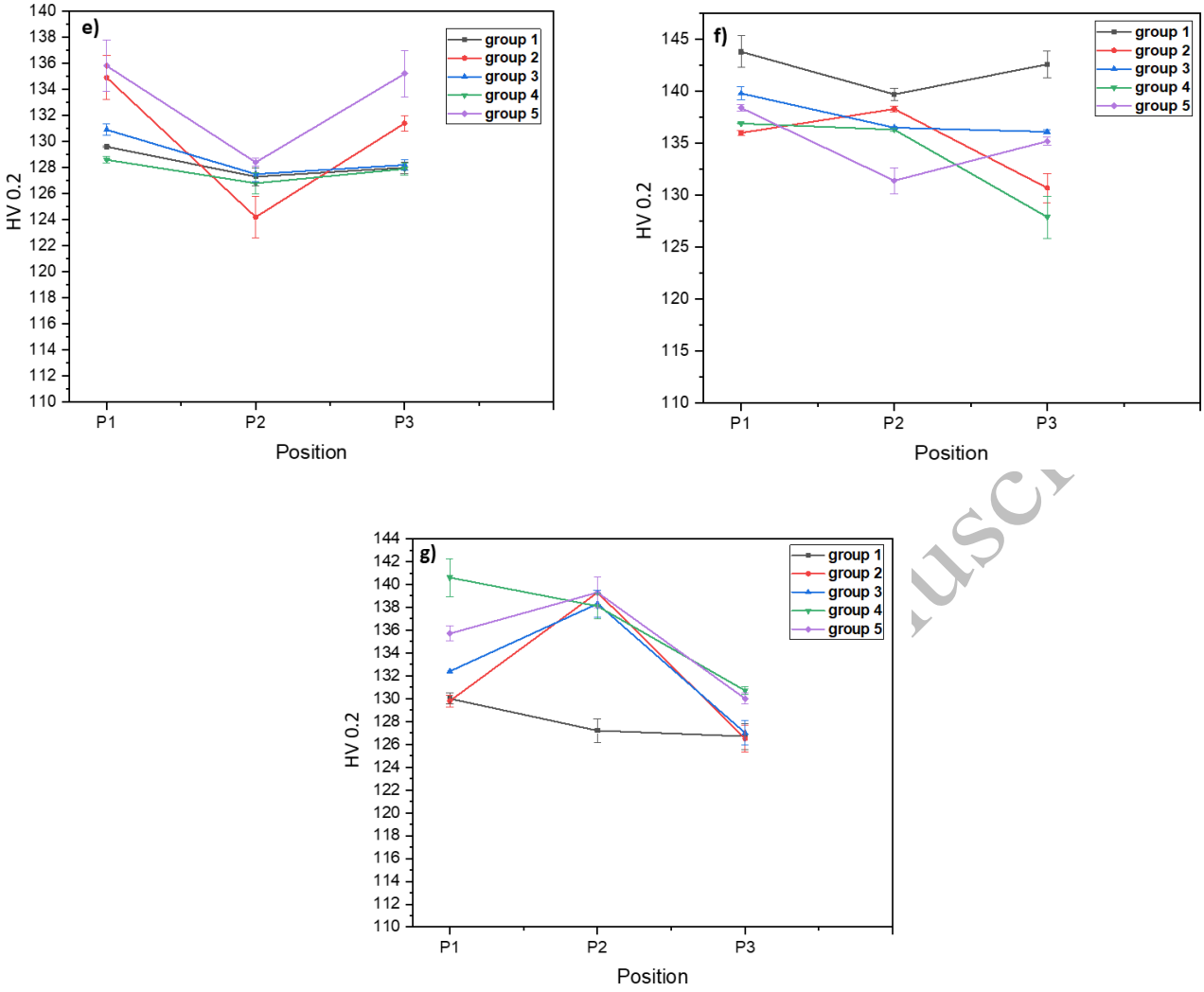

Fig. 7 microhardness and standard deviation of HV 0.2: a) before ECAP, b) S1 after ECAP, c) S2 after ECAP, d) S3 after ECAP, e) S4 after ECAP, f) S5 after ECAP, g) S6 after ECAP.

3.2 Simulation of the ECAP process:

A finite element simulation was conducted with Abaqus software to provide a better understanding of the (ECAP) process.

The simulation is employed to provide direct insights into the evolution of plastic deformation during the ECAP of multilayered DC04 steel sheets. The effective deformation in ECAP is governed by the internal and external die angles, as described by the following criterion [21]:

$$\varepsilon = \frac{2}{\sqrt{3}}\left[2\cot\left(\frac{\theta}{2}+\frac{\varphi}{2}\right)+\varphi\, cosec\left(\frac{\theta}{2}+\frac{\varphi}{2}\right)\right] \qquad (1)$$

Consequently, plunger speed has minimal influence on the deformation process. However, a low speed is used to achieve better deformation uniformity. Slower speeds promote more homogeneous deformation across the material [22], though they require longer processing times. For our purpose, the real dimensions of the different parts and the experimental conditions were respected. The parameters of mechanical properties of the material were derived from experimental data, the strain hardening is introduced using by the hollomon model

$\sigma=k.\varepsilon^n$ and the material is considered isotropic. Since the plunger and die had no deformation and had no effect on the specimen's stress state, they were taken as rigid bodies, defined as solid discrete rigid with a mesh size of 10 mm (R3D4 type: A 4-node 3-D bilinear rigid quadrilateral); the sheets are considered as deformable solid extrusion elements, with a fine mesh size of 1 mm (C3D8R type: An 8-node linear brick, reduced integration, hourglass control). The friction coefficient 0.1 following the standard Coulomb's friction law was introduced and applied between all parts of the simulation (tool/sheet contact, sheet/sheet contact and tool/tool contact), this value is literature based on the work of Alateya et al. [23], this is due to the use of lubrification during the process. The displacement of the plunger is 115 mm. Figure 8 illustrates the multilayered sample moving through the channel, providing a representation of the ECAP process from start to finish, including the Von Mises stress results of the experimental procedure.

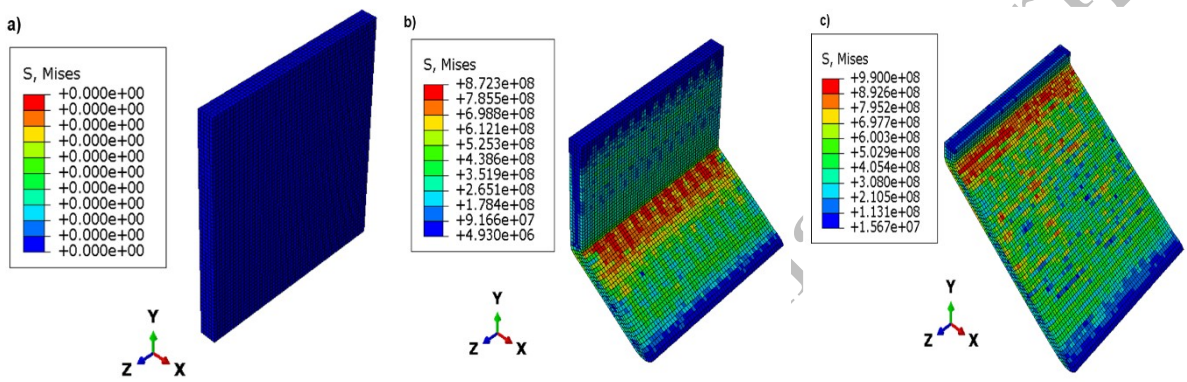

Fig. 8 ECAP simulation of DC04 sheets: a) initial state, b) middle of the simulation, c) end of the simulation.

Figure 9 shows in detail the stress distribution in the channel bend during ECAP process. The figure 9 clearly illustrates that stresses are concentrated mainly in the sheet in contact with the inside angle, while the other sheets are less affected. This observation explains the variation in micro-hardness values between S1 and the rest of the plates, highlighting that the most significant deformations are produced in plate S1. This stress concentration is also consistent with the behaviors observed in the ECAP of other bulk materials[19,21,24].

In accordance with the conclusions drawn from the microhardness results and the simulation, it seems more appropriate to concentrate our analysis exclusively on the first sheet (S1), in order to deepen our understanding of the phenomenon.

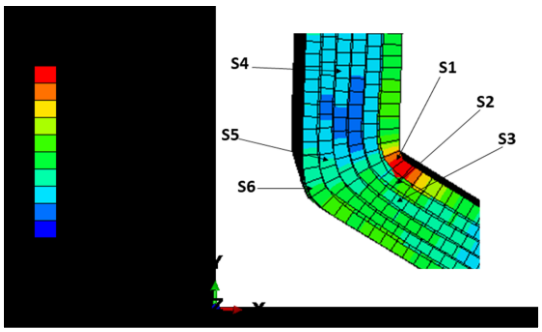

Fig. 9 distribution of stress of V. Mises during the simulation.

3.3 Effect of ECAP on microstructure:

Figure 10 shows the microstructure before and after ECAP of sheet S1, the specimens were taken from the center of the sheet represented by the location G3P2 in Fig. 4. Significant grain refinement was observed using optical microscopy, accompanied by a high density of grain boundaries (Fig. 10b). This phenomenon has also been reported by Fukuda et al. [7], M. Eddahbi et al. [9], and L. Wang et al. [26]. These optical micrographs highlighted deformation bands, indicative of the severe plastic deformation inherent to the ECAP method [10]. Additionally, the alignment of elongated grains along the shear direction suggested the development of a specific texture [27]. This grain refinement can be attributed to the severe plastic deformation generated during the pressing process through the channel, where the ferrite undergoes successive subdivision of the dislocation walls, facilitated by the operation of multi-slip systems [15,26,28-29]. The transformation from an initial coarse grain structure to a finer, more homogeneous grain distribution after ECAP is clearly demonstrated in the optical micrographs.

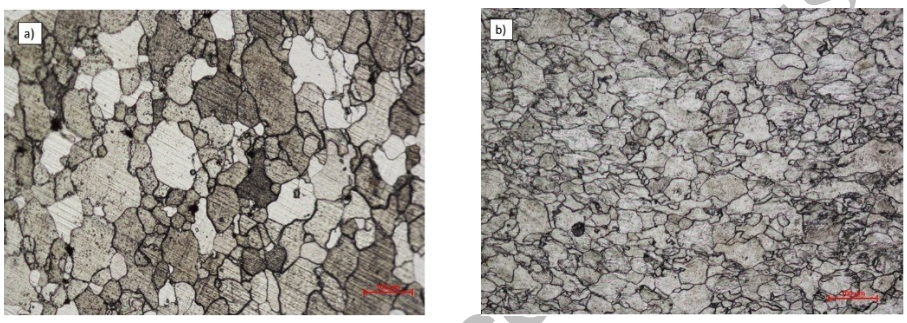

Fig. 10 Microstructure of the sheet (x100): a) before ECAP; b) S1 after ECAP.

Grain size was assessed using the intercept method, with cross and circle marks, before and after ECAP. Figure 11 illustrates the method, and the results are summarized in Table 2.

Table 3 shows a decrease of approximately 70% in the length of intersection between grain boundaries after ECAP. This finding supports the observation that grain size decreases after ECAP (Fig. 10).

Figure 12 illustrates the distribution of intersection lengths in the intercept method, before and after ECAP. Before ECAP (Fig. 12a), the distribution extends up to 600 µm, where 70% of the intersection length is concentrated between 0 and 150 µm. After ECAP (Fig. 12b), a reduction in the distribution range appears and now extends up to 120 µm, where 80% of the intersection length is concentrated between 10 and 60 µm. Thus, the homogenization of the grains size after ECAP is confirmed[9,30].

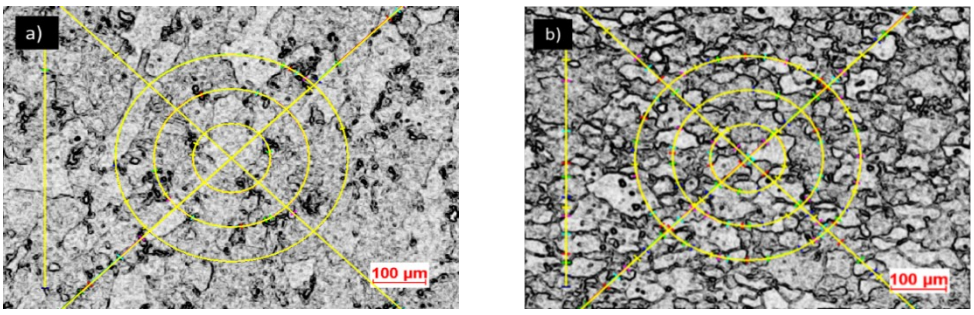

Fig. 11 Intercept method (x100): a) before ECAP; b) S1 after ECAP.

Table 2 Length of the intersection between grain boundaries and the average linear intercept in the intercept method.

	Length of intersection between grain boundaries (µm)		average linear intercept (µm)	
	Before ECAP	S1 After ECAP	Before ECAP	S1 After ECAP
Minimum	6.8	8.2		
Maximum	591.7	114.1	132.11	38.56
Mean	132.1	38.6		

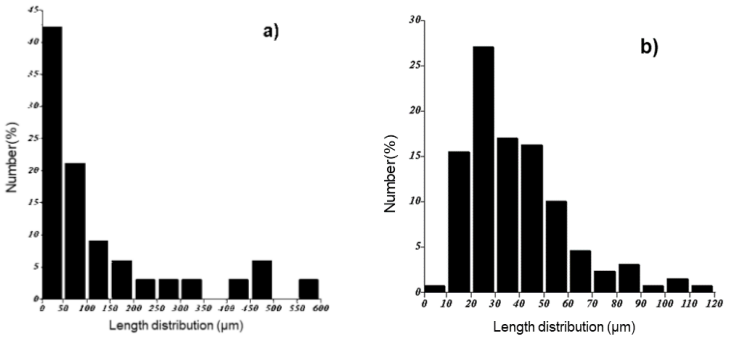

Fig. 12 Length distribution: a) Before ECAP, b) S1 after ECAP.

3.4 X-ray diffraction (XRD) analysis:

Figure 13.a illustrates the X-ray diffraction (XRD) diagrams of the sheet before and after ECAP. The two diagrams show three distinct peaks at angles (2θ) of 44.9°, 65.2°, and 82.5°, attributed respectively to the crystalline planes (110), (200), and (211) of the Im-3met space group associated with the centered cubic crystalline structure (phase α), indicating that the ECAP did not cause any phase change in DC04 steel plate.

Figure 13.b shows the measured full width at half maximum (FWHM) values of the main peaks (2θ equal to 44.9°). Compared to the sample before ECAP, the FWHM of the peak after ECAP is significantly higher, indicating that the treatment caused a decrease in grain size[10,31].This corroborates the conclusions about the decrease in grain size after ECAP, previously made.

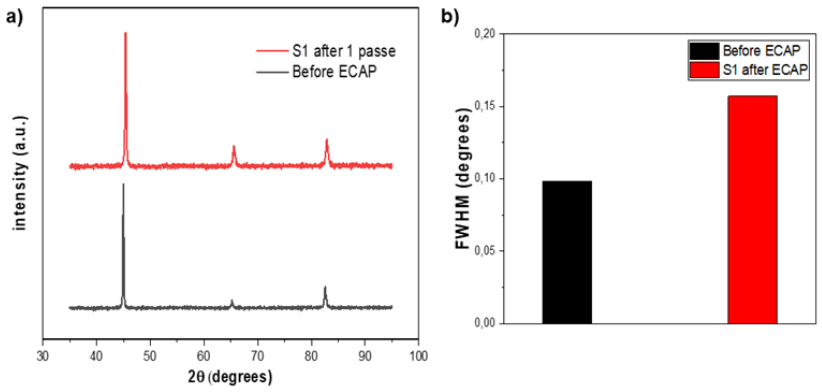

Fig. 13 a) X-ray diffraction patterns before and after ECAP; b) FWHM values.

3.5 Effect of ECAP on mechanical properties:

Figure 14 presents the tensile graphs of the samples before and after the ECAP. The results of the tensile tests are noted in Table 3.

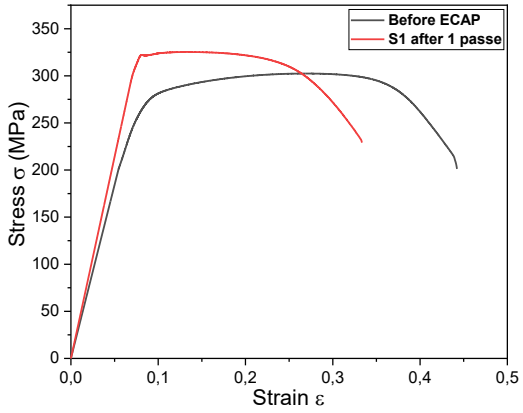

Fig. 14 Strain-stress curves before and after ECAP for S1.

Table 3 Difference in mechanical proprieties before and after ECAP for Sheet 1.

Proprieties	Re /MPa	Rm /MPa	A%	n	K
Before ECAP	267	300	37	0.23	532.8
S1 after ECAP	320	325	27	0.12	478.6

Table 4 shows an increase in yield strength (Re) and maximum strength (Rm) of 20% and 8.3%, respectively. Furthermore, a reduction of 27%, 10.17%, and 52.17% were noted in elongation (A%), the strain hardening coefficient (K), and the work hardening coefficient (n), respectively was noted. Similar behaviors have been reported in the literature[13,22,32]. These changes can result from several factors, such as the decrease in grain size and the increase in dislocation density [34].

3.6 Effect of ECAP on drawability:

Figure 15 shows the method of measuring the deformation depth of samples after Erichsen testing using a caliper. Figure 16 shows the crack in the plates after the Erichsen test. Table 4 presents the results of the Erichsen test.

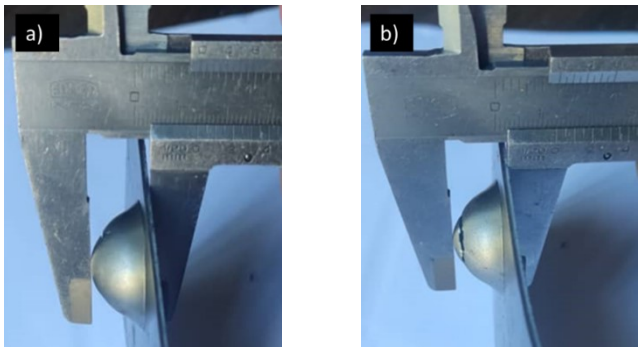

Fig. 15 Method of measuring the deformation depth of the cup: a) before ECAP; b) after ECAP.

Fig. 16 Plate cracking after Erichsen test: a) before ECAP; b) after ECAP

Table 4 Erichsen test results

	Initial steel sheet thickness /mm	Depth of the cup/mm	average IE /mm	Load /KN
Before ECAP	1.5	13.3	11.8	12.3
S1 after ECAP	1.5	12.1	10.6	14.2

After ECAP, a 10.2% decrease in the IE parameter was noted. This reduction is consistent with the results of the tensile tests carried out. Despite this reduction, it should be noted that the sheets have retained a good suitability for stamping. Figure 16 further supports this point, revealing the presence of concentric cracks in the sheets not subjected to ECAP, and subjected to ECAP. This observation serves as a secondary indicator confirming the suitability of the material for deep drawing processes after ECAP [25]. It can be noted that the tensile test revealed a work hardening coefficient (n) reduced by more than 50% after ECAP. However, the sheet maintained a good drawability. Consequently, the work hardening coefficient does not seem to be a reliable indicator of the drawability of the sheet.

The reduction in the Erichsen Index (IE) can be attributed to the elongation of grains observed through optical microscopy. These elongated grain boundaries act as preferential sites for the initiation and propagation of cracks during deep drawing processes, leading to a decrease in formability [35]. This finding contradicts tensile test results, which often show improved strength and ductility due to grain refinement. Saray et al. [36] observed similar outcomes in their study on the formability of Interstitial-Free (IF) steels, where severe plastic deformation (SPD) techniques like ECAP enhanced tensile properties but reduced formability as measured by the Erichsen test [10]. The difference arises because tensile tests measure uniaxial stress, whereas deep drawing involves complex multi-axial stresses that exploit the weaknesses introduced by grain elongation. Furthermore, while ECAP significantly refines the grain structure, leading to enhanced strength, it often results in a decrease in ductility. This reduction can be attributed to several factors: grain elongation, high dislocation density, and the presence of non-equilibrium grain boundaries [26,28,29]. These factors collectively reduce the material's ability to accommodate further plastic deformation.

3.7 Surfaces and sub-surfaces after Erichsen testing:

Figure 17 shows an overview of the different deformation zones that the sheets underwent after the Erichsen tests. It is observed that the deep drawing process generated the formation of three clearly demarcated zones, designated respectively as zone A, zone B, and zone C, each exhibiting a distinct surface morphology. We see that the surface morphologies are the same for the two samples; these areas are shown in fig. 17.a and fig. 17.b. Zone A is formed under the effect of friction forces between the punch and the sheet metal, it has a rather smooth surface. Zone B is stretched under the influence of biaxial tensile loads, it presents the roughest

surface due to the concentration of deformation bands. Zone C is deformed with biaxial bending loads, it presents a smooth surface, which indicates that this zone does not undergo considerable plastic deformation. These results are explained more deeply by Saray et al [36].

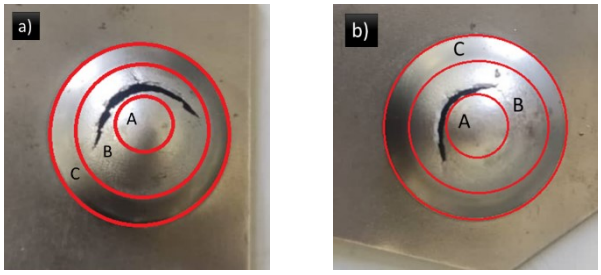

Fig. 17 different deformation zones that the sheets underwent after the Erichsen tests: a) before ECAP, b) S1 after ECAP.

3.8 Simulation of the Erichsen tests:

The numerical simulation of the Erichsen tests was carried out using Abaqus software to study the concentration of strains during these tests, before and after ECAP. In this simulation model, the die, the blank holder, and the punch are considered rigid elements and modeled as discrete rigid solid elements, the sheets are modeled as isotropic deformable element and modeled in solid deformable shell, The mesh of rigid parts (tools) is defined by the R3D4 type, while the blank is defined by S4R. The displacement of the punch into the die is 40 mm. The choice of the blank holder force and the choice of the friction coefficient has been the subject of several studies that give a balance between them [37]. For our work, the blank-holder force applied is 1.3 kN, which is measured by the Ericksen test machine. The coefficient of friction between the tools and the sheet is assumed to be 0.15 considering the dimension used. This simulation of the erichsen test and the concentration of strains are shown in Figure 18. We observe similar strain concentration in the two sheets; the highest strains are located in zone B, which corresponds to the breaking point of the sheets. This result is the same as that obtained for the experimental tests in figure 17. Lower strains are recorded in zone A, and negligible strains are recorded in zone C.

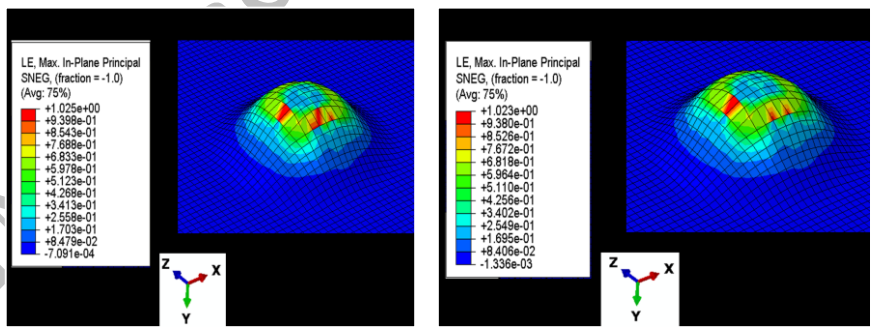

Fig. 18 simulation of the Erichsen tests of sheets: a) before ECAP, b) S1 after ECAP

The true strain/thickness graph has been plotted for both scenarios, focusing on the node exhibiting the highest strain in each simulation. The plot is shown in Figure 19. It was observed that the deformation of S1 after ECAP initiates later than that of the as-received sheet, as evidenced by the initial reduction in thickness. However, Sheet 1 reaches a thickness of 0 mm at a lower strain, indicating the onset of cracking. These simulation results align with experimental findings, which demonstrate a reduction in the Erichsen Index (IE) factor during the Erichsen test.

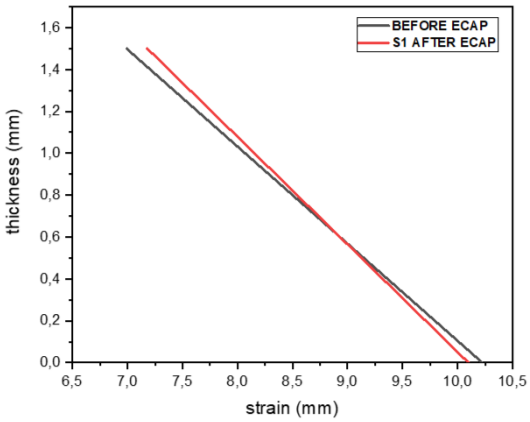

Fig. 19 The true strain/thickness graph for sheet before ECAP and S1 after ECAP

3.9 Load-displacement curves during the Erichsen tests:

Figure 20 illustrates the load-displacement curve of the punch during stamping for the two sheets (before and after ECAP for S1) as obtained from the simulation. We observe that the maximum punch load required to deform Sheet 1 after ECAP (14.103 kN) is greater than that required to deform the sheet before ECAP (12.103 kN), with the maximum load indicated by point a. This increase is attributed to the homogenization of the structure due to grain refinement (discussed in section 3.3) and the increase in microhardness (shown in section 3.1) after ECAP. These findings are also supported by Ciemiorek et al. [14]. Beyond this point, there is a reduction in the punch load, which results from the initiation and propagation of cracking. The reduction in load provides insights into the nature of sheet failure during deep drawing [38]. For sheet S1 after ECAP, analysis begins at point b, which represents the actual point of crack initiation, as evidenced by the quantitative analysis of Kamikawa et al. [39] .Comparing the behavior of segments a-c (before ECAP) and b-c (S1 after ECAP), we observe that the reduction in punch load is more rapid after ECAP, indicating that the sheet's behavior post-ECAP is less ductile due to the increase in microhardness. The results of this simulation correlate with the experimental results.

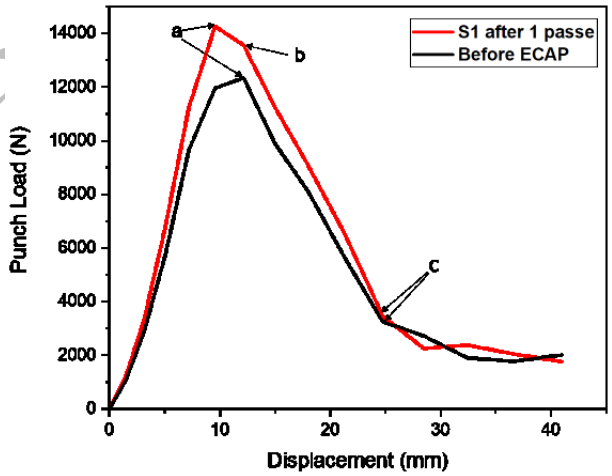

Fig. 20 representation of the punch load (N)-Displacement (mm) curve.

Conclusion:

This experimental work studies the effect of equal channel angular pressing (ECAP) on the drawability of multilayered DC04 steel sheets. The ECAP die used has a channel with an interior angle of Φ=120° and an exterior angle of Ψ=10°. The main conclusions drawn from this study are as follows:

1) The study demonstrated significant improvements in microhardness for the inner layer of the ECAP-extruded material, increasing from 120 to 197.4 HV (64%), with slight increases observed in other layers. The decrease in the standard deviation of microhardness measurements after ECAP indicates improved structural homogeneity. Finite element simulations using Abaqus showed a non-uniform stress distribution during ECAP, with the maximum stress concentrated on the inner layer.
2) Microstructural analysis revealed a 70% reduction in average grain size for the inner layer, resulting in a more uniform structure with slight texture. X-ray diffraction confirmed this grain size reduction without any phase changes. Tensile tests indicated increases in yield stress by 20% and ultimate tensile strength by 8.3%, while plastic elongation, strain hardening exponent, and strain hardening exponent decreased by 27%, 10.17%, and 52.17%, respectively.
3) The Erichsen test results showed a 10.2% reduction in the Erichsen Index after ECAP, consistent with maintaining good drawability, with cracks forming in an arc shape both before and after ECAP. No correlation between the work hardening coefficient and the IE parameter was found. Simulation insights from the Erichsen tests revealed three distinct stress zones and highlighted the less ductile behavior of the material after ECAP.

Acknowledgements

The authors would like to thank the SIDER El-Hadjar steel complex in Annaba, Annaba, Algeria, for providing the materials, as well as the Department of Metallurgy at the National higher School of Mines and Metallurgy, Annaba, Algeria, for providing the equipment when carrying out this work.

Author contribution

The study design and drafting of the manuscript were realized by all authors. The material preparation, data collection, and analysis were carried out by Massil Talantikite, Abdelmalek Mebarek, Mohamed Zaaf and Saida Boukeffa. All authors have read and approved the final manuscript.

Funding

The authors declare that no funds, grants, or other support were received during the preparation of this manuscript.

Declarations

Conflict of interest The authors declare no competing interest.

Reference:

[1] A. Atrian, F. Fereshteh-Saniee, Deep drawing process of steel/brass laminated sheets, Composites Part B: Engineering, 47 (2013) 75-81. https://doi.org/10.1016/j.compositesb.2012.10.023
[2] R. Dwivedi, G. Agnihotri, Study of deep drawing process parameters, Materials Today: Proceedings, 4 (2) (2017) 820-826. https://doi.org/10.1016/j.matpr.2017.01.091
[3] R. Z. Valiev, T. G. Langdon, Principles of equal-channel angular pressing as a processing tool for grain refinement, Progress in Materials Science, 51 (7) (2006) 881-981. https://doi.org/10.1016/j.pmatsci.2006.02.003
[4] T. G. Langdon, The Principles of grain refinement in equal-channel angular pressing, Materials Science and Engineering: A, 462 (1-2) (2007) 3-11. https://doi.org/10.1016/j.msea.2006.02.473.
[5] A. Mulay, B. S. Ben, S. Ismail, A. Kocanda, Performance evaluation of high-speed incremental sheet forming technology for AA5754 H22 aluminum and DC04 steel sheets, Archives of Civil and Mechanical Engineering, 8 (2018). https://doi.org/10.1016/j.acme.2018.03.004
[6] M. Szewczyk, K. Szwajka, The use of non-edible green oils to lubricate DC04 steel sheets in sheet metal forming process, Lubricants (2022) 1-17. https://doi.org/10.3390/lubricants10090210
[7] Y. Fukuda, K. Oh-ishi, Z. Horita, T. G. Langdon, Processing of a low-carbon steel by equal-channel angular pressing, Acta Materialia, 50 (2002) 1359-1368. https://doi.org/10.1016/S1359-6454(01)00441-4.
[8] C. S. Kondaveeti, S. P. Sunkavalli, D. Undi, L. V. Hanuma Kumar, K. Gudimetla, B. Ravisankar, Metallurgical and mechanical properties of mild steel processed by equal channel angular pressing (ECAP), Transactions of the Indian Institute of Metals, 70 (1) (2017) 83-87. https://doi.org/10.1016/S1359-6454(01)00441-4.
[9] M. Eddahbi, M. A. Monge, T. Leguey, P. Fernández, R. Pareja, Texture and mechanical properties of EUROFER 97 steel processed by ECAP, Materials Science and Engineering: A, 528 (18) (2011) 5927-5934. https://doi.org/10.1016/j.msea.2011.04.006
[10] M. B. Jabłońska, K. Kowalczyk, M. Tkocz, R. Chulist, K. Rodak, I. Bednarczyk, A. Cichański, The effect of severe plastic deformation on the if steel properties, evolution of structure and crystallographic texture after dual rolls equal channel extrusion deformation, Archives of Civil and Mechanical Engineering, 21 (4) (2021) 1-10. https://doi.org/10.1007/s43452-021-00303-6
[11] K. Kowalczyk, M. B. Jabłońska, M. Tkocz, R. Chulist, I. Bednarczyk, T. Rzychoń, Effect of the number of passes on grain refinement, texture and properties of DC01 steel strip processed by the novel hybrid SPD method, Archives of Civil and Mechanical Engineering, 22 (3) (2022) 1-12. https://doi.org/10.1007/s43452-022-00432-6
[12] J. Suh, J. Victoria-Hernández, D. Letzig, R. Golle, Effect of processing route on texture and cold formability of AZ31 Mg alloy sheets processed by ECAP, Materials Science and Engineering: A, 669 (2016) 159-170. https://doi.org/10.1016/j.msea.2016.05.027
[13] H. R. Rahimi, M. Sedighi, R. Hashemi, Forming limit diagrams of fine-grained Al 5083 produced by equal channel angular rolling process, Journal of Materials Processing Technology, 232 (2018) 922-930. https://doi.org/10.1177/1464420716655560.

[14] M. Ciemiorek, M. Lewandowska, L. Olejnik, Microstructure, Tensile properties and formability of ultrafine-grained Al–Mn square plates processed by incremental ECAP, Materials & Design, 196 (2020) 0-10. https://doi.org/10.1016/j.matdes.2020.109125
[15] M. C. V. Vega, R. E. Bolmaro, M. Ferrante, V. L. Sordi, A. M. Kliauga, The Influence of deformation path on strain characteristics of AA1050 aluminium processed by equal-channel angular pressing followed by rolling, Materials Science and Engineering: A, 646 (2015) 154-162. https://doi.org/10.1016/j.msea.2015.07.083
[16] D. M. Marulanda, J. G. Cortés, M. A. Pérez, G. García, Microstructure and mechanical properties of AISI 8620 steel processed by ECAP, Materials Research Society Symposium Proceedings, 1611 (2014) 89-94. https://doi.org/10.1557/opl.2014.763
[17] F. S. Sorce, S. Ngo, C. Lowe, A. C. Taylor, Quantification of coating surface strains in erichsen cupping tests, Journal of Materials Science, 54 (10) (2019) 7997-8009. https://doi.org/10.1007/s10853-019-03392-0
[18] J. Coër, J. C. Mise, A. Génie, Mise en forme par emboutissage en température d'un alliage d'aluminium AA5754-O (Sheet metal forming in temperature of an aluminium alloy AA5754-O), Génie mécanique [physics.class-ph], Université de Bretagne Sud, 2013, pp, 107-113. (in French).
[19] O. Hilšer, S. Rusz, M. Salajka, L. Čížek, Evaluation of the deep-drawing steel sheets processed by DRECE device, Archives of Materials Science and Engineering, 68 (1) (2014) 31-35. http://www.amse.acmsse.h2.pl/vol68_1/6815.pdf
[20] M. Ciemiorek, W. Chrominski, L. Olejnik, M. Lewandowska, Evaluation of mechanical properties and anisotropy of ultra-fine grained 1050 aluminum sheets produced by incremental ECAP, Materials & Design, 130 (2017) 392–402. https://doi.org/10.1016/j.matdes.2017.05.069
[21] R. Melicher, Numerical simulation of plastic deformation of aluminium workpiece induced by ECAP technology, Applied and Computational Mechanics, 3 (2009) 319–330. https://core.ac.uk/reader/295549020
[22] P. B. Berbon, M. Furukawa, Z. Horita, M. Nemoto,T, G. Langdon, Influence of pressing speed on microstructural development in equal-channel angular pressing, Materials Science Forum, 30 (1999) 1989–1997, https://doi.org/10.1007/s11661-999-0009-9
[23] M. O. Alateyah, M. M. Z. Ahmed, W. H. El-Garaihy, Y. Zedan, H. Abd El-Hafez, Experimental and Numerical Investigation of the ECAP processed copper: microstructural evolution, crystallographic texture and hardness homogeneity, Metals, 11(4) (2021) 607. https://doi.org/10.3390/met11040607.
[24] T. Suo, Y. Li, Y. Guo, Y. Liu, The simulation of deformation distribution during ECAP using 3D finite element method, Materials Science and Engineering: A, 432 (2006) 269–274. https://doi.org/10.1016/j.msea.2006.06.035.
[25] B. H. Shahmir, M. Nili-ahmadabadi, M. Mansouri-arani, A. Khajezade, T. G. Langdon, Evaluating the room temperature ECAP processing of a NiTi alloy via simulation and experiments, Advanced Engineering Materials, 16 (3) (2014) 224-230. https://doi.org/10.1002/adem.201400248.
[26] L. Wang, J. A. Benito, J. Calvo, J. M. Cabrera, Equal channel angular pressing of a TWIP steel: microstructure and mechanical response, Journal of Materials Science, 52 (11) (2017) 6291–6309. https://doi.org/10.1007/s10853-017-0862-7.

[27] D. Bhuyan, T. N. Rao, V. R. Reddy, A. Srinivasa, K. V. Rajkumar, Recovery of ductility in ultrafine-grained low carbon steel processed by electropulsing, Metallurgical and Materials Transactions A, 52 (7) (2021) 2992–3006. https://doi.org/10.1007/s11661-021-06293-7.
[28] L. Chen, F. P. Yuan, P. Jiang, X. L. Wu, Mechanical properties and nanostructures in a duplex stainless steel subjected to equal channel angular pressing, Materials Science and Engineering: A, 551 (2012) 154–159. https://doi.org/10.1016/j.msea.2012.04.112.
[29] V. Shivam, D. Bhuyan, N. K. Mukhopadhyay, R. Manna, Microstructural refinement and mechanical properties of ferritic stainless steel processed by equal-channel angular pressing, Journal of Materials Engineering and Performance, 29 (10) (2020) 6818–6830. https://doi.org/10.1007/s11665-020-05131-y.
[30] M. N. da Silva Lima, S. F. Rodrigues, M. Al-Maharbi, J. C. Muñoz, J. M. Cabrera Marrero, H. F. Gomes de Abreu, Effect of ECAP processing temperature on an austenitic TWIP steel's microstructure, texture and mechanical properties, Journal of Materials Research and Technology, 24 (2023) 1757–1775. https://doi.org/10.1016/j.jmrt.2023.03.116.
[31] C. Gennari, L. Pezzato, N. Llorca-Isern, A. Biserova-Tahchieva, I. Calliari, Effect of severe plastic deformation on microstructure and properties of duplex stainless steel, Materials Research Proceedings, 32 (2023) 205–212. https://doi.org/10.21741/9781644902615-23.
[32] S. Attabi, A. Himour, L. Laouar, Mechanical and wear behaviors of 316L stainless steel after ball burnishing treatment, Journal of Materials Research and Technology, 15 (2021) 3255–3267. https://doi.org/10.1016/j.jmrt.2021.09.081.
[33] A. E. Tekkaya, P. O. Bouchard, S. Bruschi, C. C. Tasan, Damage in metal forming, CIRP Annals, 69 (2) (2020) 600–623. https://doi.org/10.1016/j.cirp.2020.05.005.
[34] X. Yang, Z. Wang, Y. Dai, B. Li, Z. Jin, L. Luo, X. Liu, J. Wang, Evolution of microstructure, macrotexture and mechanical properties of high strength biomedical TA4 pure titanium during multi-pass ECAP, Journal of Materials Research and Technology, 28 (2024) 3976–3987. https://doi.org/10.1016/j.jmrt.2023.12.273
[35] O. M. Irfan, H. M. Omar, Influence of Grain Refinement by ECAP on mechanical and erosion corrosion properties of AISI 4130 steel: experimental and prediction approach, Metallurgical and Materials Transactions A, 50 (9) (2019) 4232–4244. https://doi.org/10.1007/s11661-019-05339-1.
[36] O. Saray, G. Purcek, I. Karaman, H. J. Maier, Formability of ultrafine-grained interstitial-free steels, Metallurgical and Materials Transactions A, 44 (9) (2013) 4194–4206. https://doi.org/10.1007/s11661-013-1781-0.
[37] S. Laboubi, O. Boussaid, M. Zaaf, W. Ghennai, Numerical investigation and experimental validation of Lemaitre ductile damage model for DC04 steel and application to deep drawing process, The International Journal of Advanced Manufacturing Technology, 126 (5–6) (2023) 2283–2294. https://doi.org/10.1007/s00170-023-11244-0.
[38] Y. Uriya, J. Yanagimoto, Erichsen cupping test on thermosetting CFRP sheets, International Journal of Material Forming, 10 (4) (2017) 527–534. https://doi.org/10.1007/s12289-016-1298-3.
[39] N. Kamikawa, H. Morino, Quantitative analysis of load–displacement curves in erichsen cupping test for low carbon steel sheet, Metallurgical and Materials Transactions A, 50 (11) (2019) 5023–5037. https://doi.org/10.1007/s11661-019-05418-3.